



THZ1 reveals CDK7-dependent transcriptional addictions in pancreatic cancer

Ping Lu¹ · Jing Geng¹ · Lei Zhang² · Yu Wang³ · Ningning Niu¹ · Yuan Fang⁴ · Fang Liu² · Juanjuan Shi¹ · Zhi-Gang Zhang⁵ · Yong-Wei Sun⁶ · Li-Wei Wang^{3,5} · Yujie Tang² · Jing Xue¹

Received: 5 May 2018 / Revised: 27 October 2018 / Accepted: 4 January 2019 / Published online: 28 January 2019
© Springer Nature Limited 2019

Abstract

Pancreatic ductal adenocarcinoma (PDAC) is a lethal malignancy with high mortality. Lack of effective treatment makes novel therapeutic discovery an urgent demand in PDAC research. By screening an epigenetic-related compound library, we identified THZ1, a covalent inhibitor of CDK7, as a promising candidate. Multiple long-established and patient-derived PDAC cell lines (PDC) were used to validate the efficacy of THZ1 *in vitro*. In addition, patient-derived xenograft (PDX) models and animal models of PDAC were utilized for examining THZ1 efficacy *in vivo*. Furthermore, RNA-Seq analysis was performed to reveal the molecular mechanism of THZ1 treatment. Finally, PDAC cell lines with primary or acquired resistance to THZ1 were investigated to explore the potential mechanism of THZ1 susceptibility. CDK7 inhibition was identified as a selective and potent therapeutic strategy for PDAC progression in multiple preclinical models. Mechanistic analyses revealed that CDK7 inhibition led to a pronounced downregulation of gene transcription, with a preferential repression of mitotic cell cycle and NF-κB signaling-related transcripts. MYC transcriptional was found to be involved in susceptibility of PDAC cells to CDK7 inhibition. In conclusion, Identification of CDK7-dependent transcriptional addiction in PDACs provides a potent therapeutic strategy that targets highly aggressive pancreatic cancer.

Introduction

Pancreatic ductal adenocarcinoma (PDAC), representing more than 95% pancreatic cancer, is an aggressive malignancy with high mortality. Owing to growing incidence,

late diagnosis and therapeutic insufficiency, PDAC has been predicted to become the second most prevalent cancer killer by 2020 [1]. Pancreatic cancer harbors high genetic heterogeneity [2–4], which limits the development of targeted therapies. *KRAS*, *TP53*, *CDKN2A*, and *SMAD4* are recognized as most frequent drive-mutations in PDACs [5]. However, few drugs have succeeded in targeting them so far. Therefore drug discovery is an urgent demand in PDAC research [5, 6].

Targeting transcriptional addiction becomes a promising therapeutic strategy, especially for aggressive human

These authors contributed equally: Ping Lu, Jing Geng, Lei Zhang

Supplementary information The online version of this article (<https://doi.org/10.1038/s41388-019-0701-1>) contains supplementary material, which is available to authorized users.

- ✉ Li-Wei Wang
liweiwang@shsmu.edu.cn
- ✉ Yujie Tang
yujietang@shsmu.edu.cn
- ✉ Jing Xue
jingxue@sjtu.edu.cn

¹ State Key Laboratory of Oncogenes and Related Genes, Stem Cell Research Center, Renji Hospital, School of Medicine, Shanghai Jiao Tong University, Shanghai, China

² Key Laboratory of Cell Differentiation and Apoptosis of National Ministry of Education, Department of Pathophysiology, School of

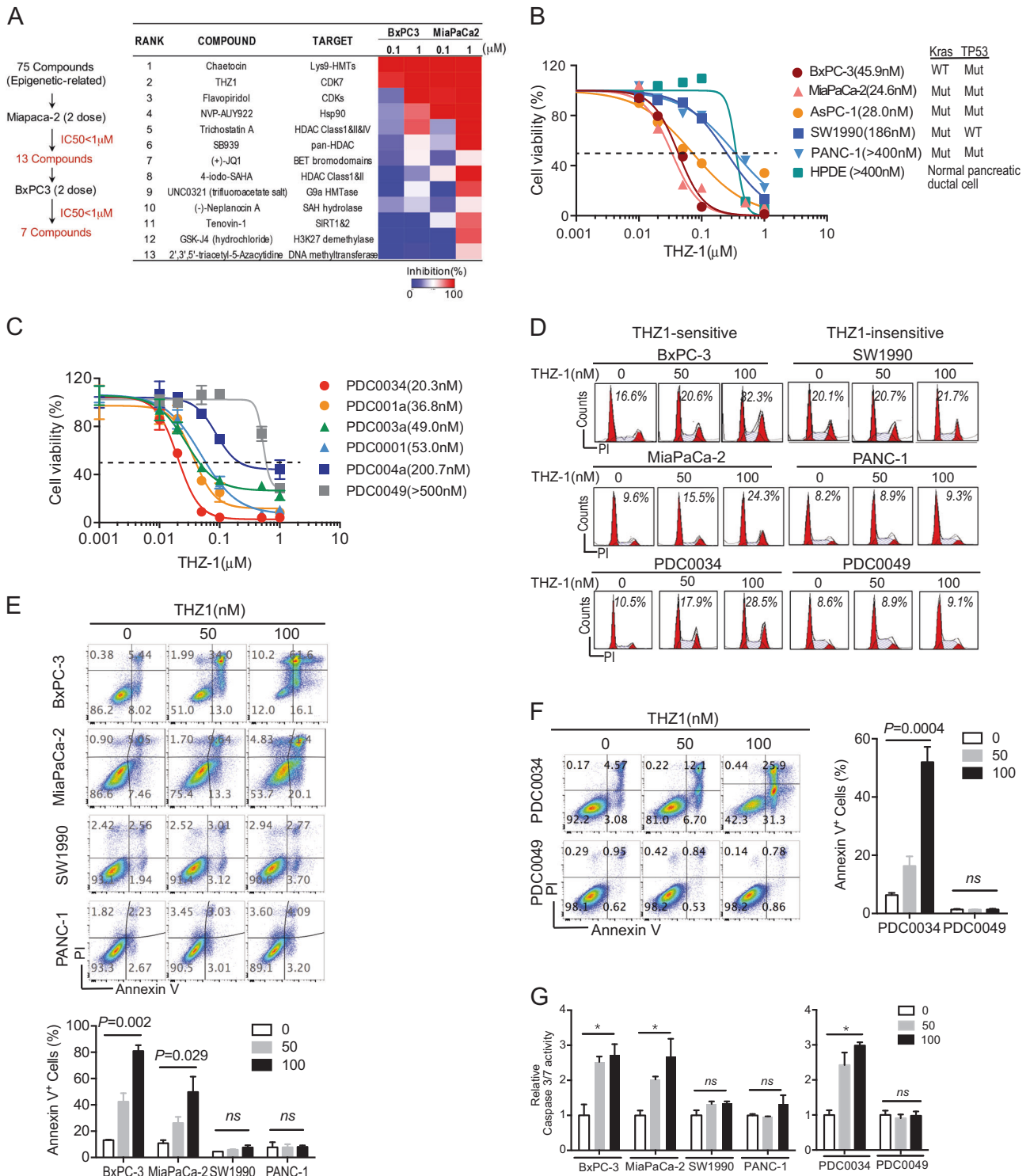
Medicine, Shanghai Jiao Tong University, Shanghai, China

³ Department of Oncology, Renji Hospital, School of Medicine, Shanghai Jiao Tong University, Shanghai, China

⁴ Research Institute of Pancreatic Disease, Ruijin Hospital, School of Medicine, Shanghai Jiao Tong University, Shanghai, China

⁵ State Key Laboratory of Oncogenes and Related Genes, Shanghai Cancer Institute, Renji Hospital, School of Medicine, Shanghai Jiao Tong University, Shanghai, China

⁶ Department of Biliary-Pancreatic Surgery, Renji Hospital, School of Medicine, Shanghai Jiao Tong University, Shanghai, China



cancers lacking druggable targets, like triple-negative breast cancer [7]. CDK7 is a cyclin-dependent kinase (CDK) and a subunit of the multi-protein basal transcription factor TFIIF, therefore plays dual roles in cell cycle and transcription regulation. As a component of TFIIF, CDK7 plays essential roles in transcription initiation and elongation by

phosphorylating C-terminal domain (CTD) of RNA polymerase II (RNAPII) [8, 9]. THZ1, a selective CDK7 inhibitor, covalently binds to CDK7 and suppresses its kinase activity based on modification of unique cysteine residue [10]. The therapeutic effect of THZ1 was identified in several types of cancers, including T-cell acute

◀ **Fig. 1** CDK7 is identified as a potent target for pancreatic cancer. **a** Schematic overview of screening of epigenetic modulators in BxPC-3 and MiaPaCa-2 (left panel). All compounds were added to cells at the concentration of 0.1 and 1 μ M, and cell viability was measured at 72 h. Compounds were then ranked based on their inhibitory effect. Top 13 ranked compounds and corresponding targets as represented in a heatmap format (right panel). **b, c** indicated PDAC cell lines **b** and PDCs **c** were exposed to increasing doses of THZ1. Percentage of cell viability relative to that of DMSO-treated cells is shown. Data represent mean \pm SD of three replicates. **d** Cell-cycle analysis of PDAC cell lines and PDCs exposed to THZ1. **d** Cell-cycle analysis of (50 nM and 100 nM for 24 h by flow cytometry with propidium iodide (PI) staining. Results are representative of three replicates. **e, f** Apoptosis analysis in PDAC cell lines **e** and PDCs **f** were treated with THZ1 as in **d** by flow cytometry with Annexin V/PI staining (Mean \pm SD, one-way ANOVA). **g** Relative caspase 3/7 activity of indicated PDAC cell lines and PCs after exposure to THZ1 for 24 h (Mean \pm SD, one-way ANOVA, * $p < 0.05$)

lymphoblastic leukemia [10], MYCN-driven neuroblastoma [11], triple-negative breast cancer [7], small cell lung cancer [12], esophageal squamous cell carcinoma [13], nasopharyngeal carcinoma [14], ovary cancer [15], and adult T-cell leukemia [16].

Epigenetic dysregulation participates in many human cancers, including PDAC. Using small-molecular screen approach, we observed that PDAC is highly sensitive to transcription targeting drugs and in particular to CDK7 inhibitor THZ1. Here we identified the therapeutic potential of THZ1 in PDAC with in vitro and preclinical in vivo models. During the progression of PDAC, the role of CDK7 has not been elucidated yet. We first revealed the CDK7-dependent transcriptional addiction existed in a subgroup of PDAC cells, as CDK7 inhibition led to a pronounced dysregulation of gene transcription. Moreover, transcriptional addiction dependence on CDK7, the expression of MYC and ABCB1 partially mediated the intrinsic and acquired resistance to THZ1. Taken together, our findings provided a promising therapeutic strategy in CDK7-addictive pancreatic cancer.

Result

CDK7 inhibitor THZ1 exhibits high potency and selectivity for pancreatic cancer

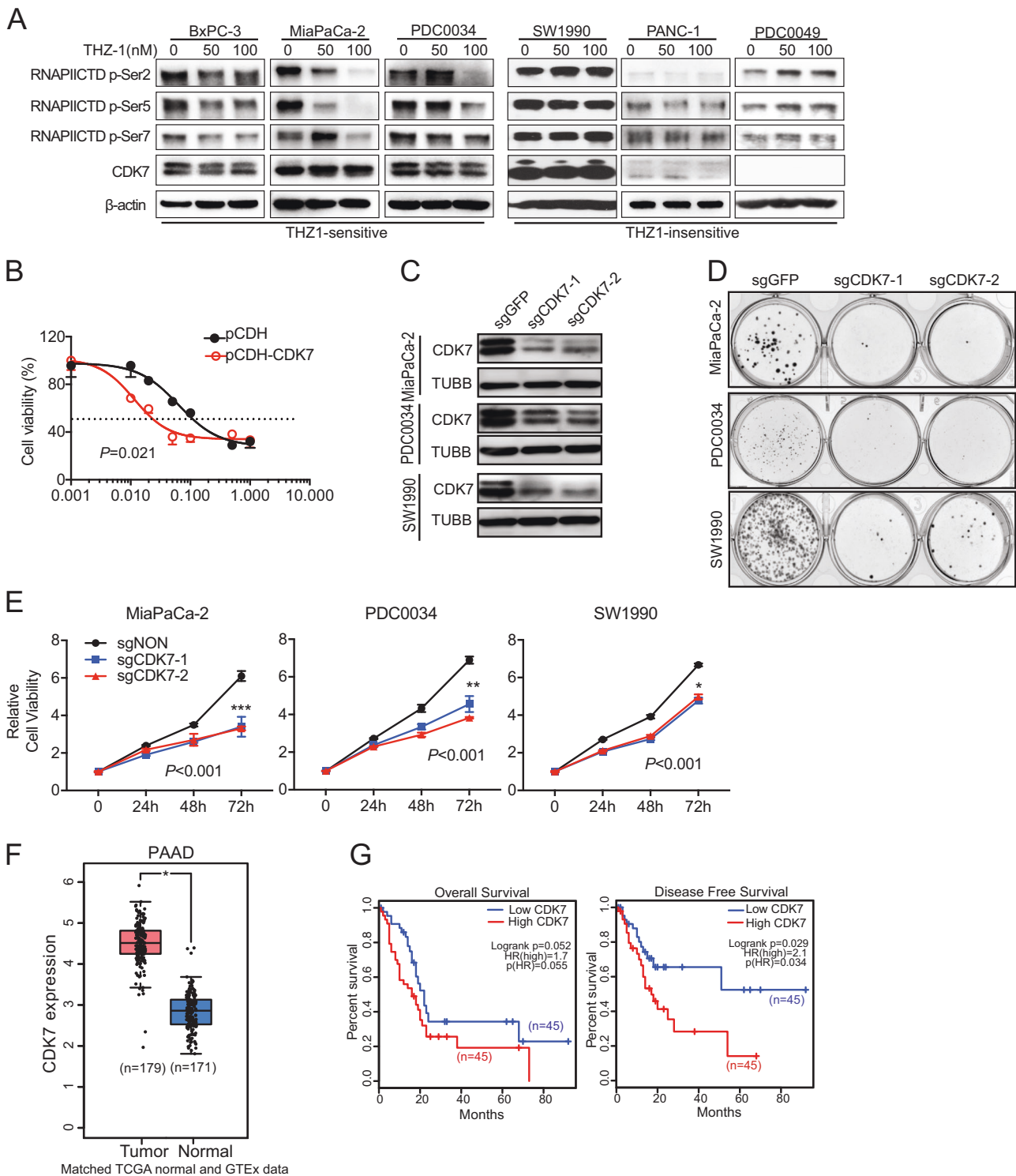
Accumulating evidences suggest that epigenetic dysregulation plays an important role in pancreatic tumorigenesis. Epigenetic drugs, such as the BET (Bromo- and Extra-Terminal) domain family of proteins or histone deacetylase inhibitors [18–20], have gained promising preclinical results in PDAC and are currently in early phases of clinical evolution. To identify more potent compounds that suppress PDAC growth, we performed a screening in PDAC cells

utilizing 75 epigenetic-related compounds (selected from a commercial Epigenetics Screening Library). To account for tumor heterogeneity, two PDAC cell lines (BxPC-3 and MiaPaCa-2) with different mutational backgrounds were subjected to screening with a cell viability assay (Fig. 1a). Thirteen compounds (for MiaPaCa-2) and seven compounds (for both cell lines) elicited reduction in growth >50% upon the concentration of 1 μ M. Four out of the seven top-ranked compounds are related to transcription (THZ1, flavopiridol, NVP-AUY922, and JQ1) (Fig. 1a). THZ1, a recently identified covalent CDK7 inhibitor, has shown a high potency against multiple cancers through targeting transcriptional addictions. The high ranking of THZ1 in our drug screen suggests the similar transcriptional addictions existing in PDAC as well.

Next, we continued to validate the suppressive effect of THZ1 on other PDAC cell lines. Here, we found THZ1 elicited much less cytotoxicity on a normal pancreatic ductal cell (HPDE), in contrast to PDAC cells. Notably, some PDAC cell lines (BxPC-3, MiaPaCa-2, and AsPC-1) were ultrasensitive to THZ1, while other PDAC cell lines (SW1990 and PANC-1) were relatively insensitive (Fig. 1b). The observed differences were not relevant to *Kras* and *Trp53* mutant status, the two major oncogenic drivers of PDAC. Similar results were obtained when THZ1 were tested against a large panel of pancreatic patient-derived cancer cells (PDCs) (Fig. 1c). Furthermore, we studied the anti-proliferative effects of THZ1. THZ1-sensitive PDACs (BxPC-3, MiaPaCa-2, and PDC0034) cells treated with THZ1 underwent cell cycle arrest in G2/M at 24 h, a phenomenon that was not observed in THZ1-insensitive PDACs (SW1990, PANC-1, and PDC0049) (Fig. 1d). Moreover, THZ1 led to a profound induction of apoptosis in THZ1-sensitive PDACs, but not in THZ1-insensitive PDACs (Fig. 1e–g). Together, these data indicate that THZ1 displays high potency and selectivity for PDAC.

CDK7 is indispensable for PDAC growth and sensitivity to THZ1

As a transcriptional kinase, CDK7 exerts its effects through regulation of RNA polymerase II-mediated transcriptional initiation and elongation. We observed that the RNAPII CTD phosphorylation was dramatically decreased in THZ1-sensitive cell lines by THZ1 treatment in a dose-dependent manner (Fig. 2a). In addition, we realized that the expression of CDK7 was extremely low in two cell lines (PANC-1 and PDC0049) compared to others, suggesting their growth independence of CDK7. Meanwhile, ectopic expression of CDK7 in PANC-1 could partially re-sensitize it to THZ1 treatment, which indicated that CDK7 independence might count for their less sensitivity to THZ1. (Fig. 2b). To further



prove the importance of CDK7 in PDAC on the cellular level, we genetically targeted CDK7 by CRISPR-Cas9 system (Fig. 2c). Downregulation of CDK7 in PDAC cells led to a significant decrease in cell growth (clone formation and proliferation), as illustrated by two THZ1-sensitive cell lines (MiaPaCa-2 and PDC0034) and one THZ1-insensitive

cell line (SW1990) (Fig. 2d, e). Unlike PANC-1 and PDC0049, the expression of CDK7 is higher and indispensable for cells growth in SW1990, indicating different mechanism contributing to its insensitivity to THZ1. Furthermore, we wonder if CDK7, is crucial to the progression of PDAC. Through GEPIA (Gene Expression Profiling

◀ **Fig. 2** CDK7 is indispensable for PDAC growth. **a** Immunoblot analysis of RNAPII CTD phosphorylation, CDK7 and β -actin in PDAC cells exposed to indicated dose of THZ1 for 6 h. **b** Cell viability comparison between CDK7-expressing (pCDH-CDK7) and control vector-expressing (pCDH) in PANC-1, after 72 h treatment with increasing doses of THZ1. Results are means \pm SD of three replicates (Two-way ANOVA). **c** PDAC cells were infected with lentivirus encoding indicated sgRNAs (sgGFP, sgCDK7-1 and sgCDK7-2). Immunoblotting for the expression of CDK7 and TUBB. **d** Cells as in **c** were seeded in 12-well plates (5000–10000 cells per well), harvested in 10 days for crystal violet staining. **e** Quantification of cell viability. Cells were treated as in **c**, then seeded in 96-well plates for cell viability assay. Cell viability relative to that of sgGFP cells is shown. Data were represented as mean \pm SD, Two-way ANOVA plus Multiple *t*-test, ****P* < 0.001, ***P* < 0.01, **P* < 0.05. **f** CDK7 expression in PDAC tissues and normal pancreas tissues. The analysis was conducted with TCGA (PAAD) and GETx (Pancreas) database. **p* < 0.05. **g** The association between CDK7 transcript level and Overall survival or Disease free survival of PDAC patients. Analyses were conducted with TCGA (PAAD) database

Interactive Analysis), we found that CDK7 is highly expressed in PDAC tissues, compared with adjacent tissues and normal pancreas tissues [21] (Fig. 2f). Moreover, the higher level of CDK7 in tumor tissues is negatively associated with PDAC patients' outcome, especially with disease free survival (Fig. 2g). Taken together, CDK7 is indispensable for PDAC progression, and its expression might partially count for sensitivity to THZ1 in PDAC.

THZ1 suppresses the growth of patient-derived xenografts from PDAC

Next, we proceeded to investigate whether CDK7 inhibition would exhibit anti-PDAC efficacy *in vivo*. Patient-derived xenografts, mimicking human tumor growth in rodent models, have been regarded as a powerful tool for drug discovery [22]. We evaluated the anti-tumor effect of CDK7 inhibition in two-independent PDX models of PDAC tumors, PDX0018 and PDX0088, whose PDAC cells have obvious CDK7 expression (Fig. 3a, b). Tumor fragments were inoculated subcutaneously into BALB/c (nu/nu) mice. When tumor grew to an average size \sim 100–150 mm³, mice were treated with THZ1 twice daily at the dose of 10 mg/kg for 16–20 days. The dose didn't give rise to overt toxicity, such as loss of body weight (Fig. 3a, b). Notably, THZ1 treatment resulted in a significant reduction of tumor volume and weight (Fig. 3a–d). Compared with vehicle-treated tumors, tumor tissues isolated from mice treated with THZ1 had reduced proliferation and increased apoptosis, as indicated by immunostaining against Ki67 and cleaved Caspase 3 (CC3), respectively (Fig. 3e, f). Apoptosis induced by THZ1 was further confirmed by significant downregulation of multiple anti-apoptotic genes, including MCL1, BIRC3, and XIAP (Fig. 3g).

THZ1 ameliorates tumor progression in spontaneous and pancreatitis-induced PDAC murine models

We further explored the *in vivo* efficacy of THZ1 using animal models. Spontaneous pancreatic carcinogenesis model, PDX^{Cre}Kras^{+LSL-G12D} (hereafter referred to as KC) and PDX^{Cre}Kras^{+LSL-G12D}Trp53^{+R172H} (hereafter termed as KPC) mice, are faithful rodent models recapitulating the characteristic of PDAC initiation and progression [23]. As we know, KC mice develop only pancreatic intraepithelial neoplasia (PanIN), while KPC mice could develop PDAC as early as 2–3 months age. As shown in Fig. 2, CDK7 played a critical role in PDAC, evidenced both by clinical investigation and cellular assays. We wonder whether CDK7 participate in the progression of KPC mice. By comparing CDK7 protein level among pancreatic lysates from PDX^{Cre}, KC and KPC mice at the age of 3 months, we found CDK7 was dramatically upregulated in KPC mice, accompanied by the induction of phosphorylation of RNAPII CTD, indicating that CDK7 involved in the tumorigenesis of KPC mice (Fig. 4a). On the basis of these observations, we examined the effect of THZ1 on KPC mice. 10-week-old KPC mice were treated with Vehicle or THZ1 (10 mg/kg twice daily) for 3 weeks. Relative pancreas weight and representative images of H&E staining of pancreas tissues illustrated that THZ1 significantly hampered PDAC progression (Fig. 4b, c). Further IHC analysis showed Ki67 expression was decreased while cleaved Caspase 3 was elevated in the pancreatic section from KPC mice treated by THZ1 (Fig. 4d).

Pancreatitis induced by hyper-stimulation of caerulein accelerates PDAC progression in KC mice by abrogating the senescence barrier in low-grade PanINs [24]. Here we found CDK7 and phosphorylation of RNAPII CTD (Ser2) were elevated in the mouse model of PDAC co-triggered by Kras activation and caerulein-induced inflammation (Fig. 4e). THZ1 treatment reduced pancreas size, pancreatic cell proliferation and the development of pancreatic malignant lesions (Fig. 4f, g). Immunoblot analysis showed decreased activation of the pro-survival kinase AKT [25, 26] as well as inflammatory mediator STAT3 [27] and p65 [28] in pancreas from THZ1-treated mice (Fig. 4h). In summary, THZ1 decreased PDAC progression both in KPC and pancreatitis-induced PDAC models.

THZ1 treatment causes global transcriptional downregulation and preferentially targets mitosis and NF- κ B-related transcripts in PDAC cells

Given the role of CDK7 in RNAPII-mediated transcription, we next compared the effect of CDK7 inhibition on overall

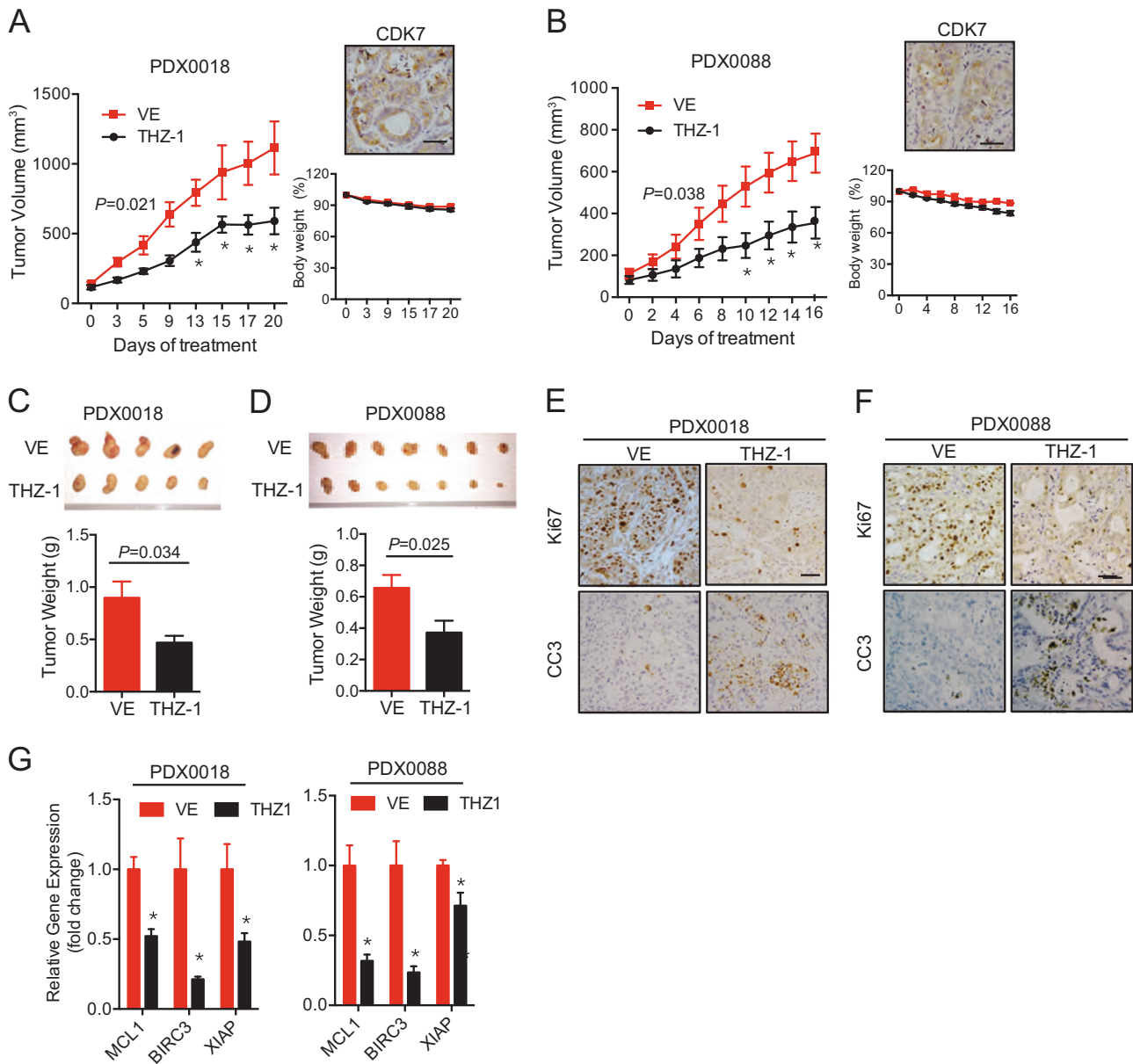
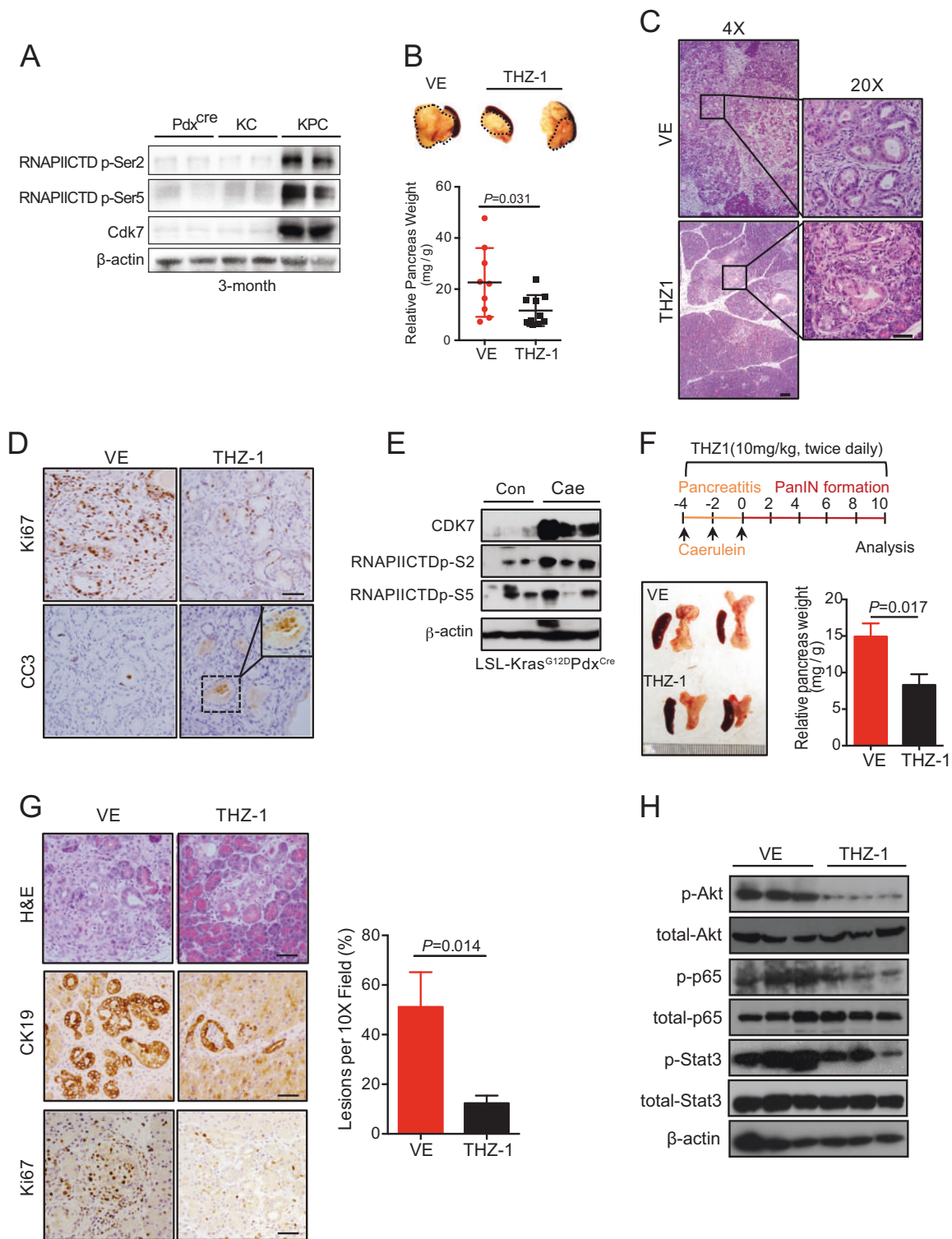


Fig. 3 THZ1 suppresses the growth of patient-derived xenografts from PDAC. **a, b** Patient-derived xenografts from PDAC tumors PDX0018 **a** and PDX0088 **b** were treated with vehicle (VE) or THZ1 (10 mg/kg body weight, twice a day) for 16–20 days. The tumor volume was monitored every 2–3 day. Mean \pm SEM, $*p < 0.05$ ($n = 5$, One-way ANOVA, Tukey’s post hoc test). **c, d** Weight of PDX0018 and PDX0088 tumors was shown (Mean \pm SEM, $n = 5$, Student’s *t*-test).

e, f Immunohistochemical (IHC) analysis of proliferation (Ki67) and apoptosis (cleaved caspase 3, CC3) in PDX0018 and PDX0088 tumors collected from A&B. Scale bar represents 50 μ M. **g** mRNA level of apoptosis-related genes (*MCL1*, *BIRC3*, and *XIAP*) were examined in PDX0018 and PDX0088 tumors collected from A&B, respectively. Mean \pm SEM, $*p < 0.05$ (unpaired Student’s *t*-test)

gene expression in THZ1-sensitive cell lines (BxPC-3 and MiaPaCa-2) versus insensitive cell lines (PANC-1) following exposure to 100 nM THZ1 for 6 h. Expression profiling was performed with spike-in RNA standards normalized to cell number to enable accurate detection of differences in total RNA levels in all samples [29]. Global downregulation of most actively transcribed genes was observed in THZ1-sensitive cell lines (BxPC-3 and MiaPaCa-2) in comparison with DMSO-treated cells, which

was not evident in THZ1-insensitive cell line PANC-1 (Fig. 5a, b). Moreover, MiaPaCa-2 and BxPC-3 cells shared a significant portion of 2960 downregulated transcripts in common, among which only 43 genes were also downregulated in PANC-1 cells (Fig. 5c). Gene ontology (GO) analysis of top 5% of downregulated transcripts revealed a significant enrichment of genes involved in transcription, DNA repair and mitotic cell-cycle checkpoint (Fig. 5d). Moreover, KEGG pathway and gene set enrichment



analysis (GSEA) showed that genes involved in multiple critical signaling pathways, TNF/NF- κ B signaling in particular, was significantly enriched in THZ1-downregulated transcripts (Fig. 5e, Figure S1). The most downregulated gene sets including mitotic cell-cycle checkpoint and NF- κ B signaling pathway displayed few changes in THZ1-

insensitive cell line (PANC-1) after exposure to THZ1 (Fig. 5f, g). PLK1 [30], CDC25 [31], and RELA [32, 33], key genes involved in mitosis and NF- κ B signaling play a critical role in PDAC progression. With TCGA database, we confirmed that the expression level of PLK1, CDC25, and RELA were associated with prognosis of PDAC

Fig. 4 THZ1 ameliorates PDAC progression in spontaneous and pancreatitis-induced PDAC mouse models. **a** Immunoblot analysis with the indicated antibodies on pancreas lysates from PDX^{cre}, PDX^{cre}Kras^{+/-LSL-G12D}(KC) and PDX^{cre} Kras^{+/-LSL-G12D}Trp53^{+/-R172H}(KPC) mice at 3 months of age. β -actin serves as a loading control. **b** KPC mice were treated with VE or THZ1 (10 mg/kg body weight, twice a day) for 4 weeks. Representative images and the relative weight of pancreas from indicated group were shown (Mean \pm SEM, $n = 9-10$, Student's t -test). **c** H&E staining of tissue sections from **b**. Images on the left and right were captured using $\times 4$ and $\times 20$ object lens, respectively. Scale bars, 100 μ m. **d** IHC analysis of Ki67 and cleaved caspase 3 (CC3) on pancreata section from VE or THZ1-treated KPC mice. Scale bars, 50 μ m. **e** Pancreatitis was induced with caerulein injection for 1 week (50 μ g/kg, 6 hourly injection per day, three times per week). Saline was injected as control. Immunoblot analysis with the indicated antibodies on pancreas lysates from control (Con) or caerulein (Cae)-treated mice. **f** Schematic of the THZ1 treatment over pancreatitis-triggered precancerous (PanINs) lesion formation in KC mice. Representative pancreas images and relative pancreas weight of VE or THZ1-treated mice are shown (mean \pm SEM, $n = 6$, Student's t -test). **g** Representative HE staining and IHC for CK19 and Ki67 in KC mice in response to THZ1 treatment. Scale bars, 50 μ m. Quantification of lesion per $\times 10$ field is shown. **h** Immunoblot analysis of indicated proteins on pancreas lysates collected from VE and THZ1-treated mice in **f**

patients (Figure S2A-C). Moreover, we found that the CDK7 expression was positively correlated with PLK1, CDC25, and RELA, respectively, (Figure S2D-F). Finally, a few THZ1-targeted cell-cycle associated genes (PLK1 and CDC25C) as well as NF- κ B signaling genes (IKKB and RELA) were further confirmed in THZ1-treated PDX0018 and PDX0088 mice (Fig. 5h). Together, THZ1 inhibited PDAC progression through globally downregulating RNAPolIII-mediated transcription, especially through triggering genes/signaling pathways indispensable for PDAC growth (Fig. 5I).

MYC is involved in THZ1 susceptibility of PDAC cells

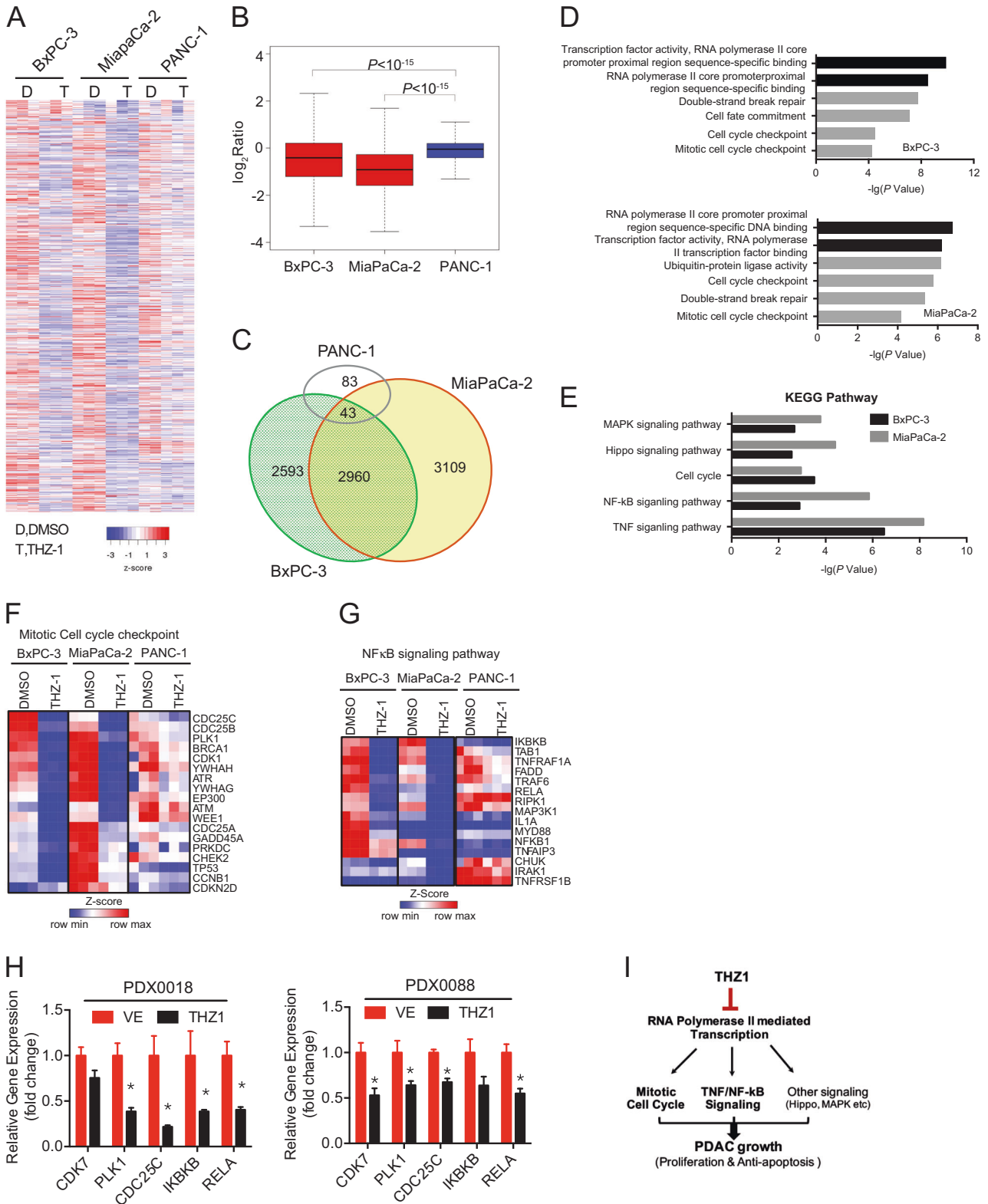
As shown in Fig. 1, PDAC cell lines vary in their susceptibility to THZ1 treatment. To explore the molecular mechanism associated with THZ1 susceptibility, we generated THZ1-resistant PDAC cell line MiaPaCa2-R by continuously exposing THZ1-sensitive cell line MiaPaCa2 to escalating doses of THZ1, until they were able to proliferate normally in the presence of 100 nM THZ1. The half maximal inhibitory concentration (IC₅₀) of MiaPaCa2-R for THZ1 was about 17 times of MiaPaCa-2 cells (Fig. 6a), and RNAPII CTD phosphorylation was much less affected upon THZ1 in MiaPaCa2-R cells compared to MiaPaCa2 (Figs. 6b, 2a). To identify crucial genes or pathways involved in susceptibility to THZ1, we performed GSEA of RNA-seq profile of MiaPaCa2-R and the parental MiaPaCa2 cells. Interestingly, a couple of MYC-downregulated gene sets were found to be enriched in MiaPaCa2-R cells, together with MYC mRNA expression downregulation

(Fig. 6c, d). Our immunoblot analyses confirmed the dramatic downregulation of MYC expression in MiaPaCa2-R cells (Fig. 6e). Given previous study [11] reported that MYCN-amplified neuroblastoma cells are more susceptible to THZ1 than non-MYCN-amplified neuroblastoma cells, we went further to test whether MYC was critical for THZ1 sensitivity in PDAC cells. Interestingly, ectopic MYC expression in MiaPaCa2-R or PANC-1 cells could resensitize them to THZ1 treatment (Fig. 6f, g). Finally, the MYC transcriptional expression of tested PDC cells and PDAC cell lines were found to be positively correlated with their susceptibilities to THZ1 (Fig. 6h). Taken together, these results indicate that MYC expression is associated with THZ1 susceptibility in PDAC cells.

Discussion

PDAC is one of the most lethal cancers to date. Lack of targeted therapy makes drug discovery of priority in PDAC research [6]. Recent efforts invested into epigenetic regulation of PDAC open new opportunity [18]. Moreover, several epigenetic-related drugs have got promising pre-clinical outcomes [18–20], which encourages us to perform a screening of compounds targeting epigenetic modulators, in search of promising anti-PDAC small molecules and additional molecular mechanisms. In this work, our in vitro epigenetic compound screening identified a covalent CDK7 inhibitor THZ1 as one of the top potent anti-PDAC agents. We further demonstrated the therapeutic efficacy of CDK7 inhibition in multiple human and mouse PDAC preclinical tumor models, proving targeting CDK7 may represent a novel selective strategy in PDAC [8].

Large-scale, deep-sequencing-based genomic analyses have revealed a high level of genetic heterogeneity in PDAC, including dominant mutations, such as Kras [3]. In spite of extreme genetic complexity, tumor cells could be addicted to an aberrant hyperactive transcription status. CDK7, the target of THZ1, plays a vital role in transcription initiation and elongation. Our results showed blockade of CDK7 by THZ1 led to a widespread transcriptional downregulation in a selective subgroup of PDAC cells, indicating transcription of these THZ1-sensitive PDAC cells were dependent on CDK7. In addition to global transcription inhibition by THZ1, our RNA-Seq analysis found the most downregulated transcripts by THZ1 were significantly related to mitotic cell cycle and NF- κ B pathway, which had been proven to be critical in the development of PDAC [28, 32]. As we known, CDK7 could regulate cell cycle by phosphorylation other CDKs. Here we found THZ1 directly downregulated transcription of cell cycle-related genes, such as PLK1 and CDC25. Here we believed that arrested cell cycle by THZ1 was mainly caused by transcription inhibition.



Of note, not all PDAC cell lines are sensitive to THZ1, indicating the existence of primary THZ1 resistance. On the other hand, acquired drug resistance to THZ1 may inevitably

arise despite the promising anti-PDAC potency of THZ1 in our preclinical tests, which was confirmed by our established THZ1-insensitive MiaPaCa2-R cells by culturing THZ1-

◀ **Fig. 5** THZ1 preferentially downregulates transcription-related genes in PDAC cells. **a** Heatmap of gene expression values in THZ1-sensitive cell lines (MiaPaCa-2 and BxPC-3) and insensitive cell line (PANC-1) treated with THZ1 (100 nM) versus DMSO for 6 h. Rows show Z-scores are calculated for each cell type. **b** Quartile box plots of log₂ fold changes in gene expression in THZ1-sensitive cell lines and an insensitive cell line treated with DMSO or THZ1 at the same dose and duration as in **a**. Box plot whiskers extend to two times the interquartile range. $P < 10^{-15}$ for BxPC-3 versus PANC-1 and MiaPaCa-2 versus PANC-1 (Two-sided Wilcoxon test). **c** Venn diagram depicting the overlap between sets of differentially expressed transcripts (THZ1 versus DMSO) in THZ1-sensitive cell lines and insensitive cell line treated with THZ1 as in **a**. **d, e** Enrichment *p*-values for selected GO functional categories and KEGG pathway of top 5% downregulated genes (versus DMSO) in BxPC-3 and MiaPaCa-2 cells following treatment with 100 nM THZ1 using DAVID software. **f, g** Heatmaps showing normalized expression of genes associated with the Mitotic cell cycle checkpoint or NF- κ B signaling pathway in BxPC-3, MiaPaCa-2, and PANC-1 cells treated with THZ1 as in **a**. Rows show Z-scores calculated for each cell type. The list of genes for each panel was extracted from GO or KEGG pathway analysis of D&E. **h** Validation of key genes sensitive to THZ1 exposure by quantitative PCR analysis in VE or THZ1-treated PDX0018 and PDX0088 tumors. Mean \pm SEM, $n = 5-7$, * $p < 0.05$ (Student's *t*-test). **i** Mechanistic scheme of anti-PDAC effects of THZ1

sensitive MiaPaCa2 with increasing sub-lethal doses of THZ1. Here we found the expression of MYC (both mRNA and protein level) was downregulated dramatically in MiaPaCa2-R cells, might attribute to genomic loss of MYC (Figure S4). Considering MYC is a critical target of THZ1 in PDAC (Figure S3), we speculate that downregulation of MYC may happen as part of adaptive response to targeted cancer therapy during the long-term THZ1 treatment at sub-lethal dose, until these cells become THZ1 resistant and MYC independent. In addition, we observed that the expression of MYC in the primary THZ1-insensitive cell lines (PANC1 and PDC0049) was at a very low level (Figure S4A). By ectopically expressing MYC in MiaPaCa2-R or PANC1 cells, we found that MYC might be involved in PDAC resistance to THZ1. Furthermore, regression analysis confirmed the positive relationship between MYC expression and the sensitivity of PDAC to THZ1. Thus, detecting the expression of MYC in patients' tumor might help guide the enrollment of patients for THZ1 treatment.

Notably, a recent study disclosed upregulation of multi-drug transporters ABCB1 and ABCG2 transcripts as a mechanism of acquired resistance to THZ1 in neuroblastoma and lung cancer, respectively [34]. To investigate whether there is a similar mechanism of THZ1 resistance in PDAC, we investigated the gene expression profiles among THZ1-sensitive PDAC cells and cells with either primary or acquired THZ1 resistance. Consistent with previous report, the expression of ABCB1 and ABCG2 was elevated in acquired THZ1-resistant cell (MiaPaCa2-R) and primary THZ1-resistant cell with high expression of CDK7 and MYC (SW1990). Furthermore, by using antagonists of

ABCB1 and ABCG2, we found that inhibition of ABCB1 could largely re-sensitive MiaPaCa2-R and SW1990 to THZ1 (Figure S5). Altogether, ABCB1 upregulation is one of the mechanism of PDAC resistance to THZ1.

In summary, we have discovered a CDK7-dependent transcriptional addiction in pancreatic cancer and identified CDK7 inhibitor THZ1 as a highly selective and potent means to target progression of pancreatic cancer.

Materials and methods

Compounds

The compounds for screening are selected from Epigenetics Screening Library (No.11076, Cayman Chemical). THZ1 (HY-80013) was purchased from MedChem Express.

Cell culture

Human pancreatic cancer cell lines (BxPC-3, MiaPaCa-2, SW1990, PANC-1, ASPC-1) and human pancreatic epithelial cell line HPDE6-C7 were obtained from ATCC. Above cells were cultured in RPMI1640 or DMEM medium supplemented with 10% fetal bovine serum (FBS) and 1% penicillin/streptomycin. Pancreatic patient-derived tumor cells (PDCs) including PDC0001, PDC0034, PDC0049, PDC001a, PDC003a, and PDC004a were isolated from pancreatic PDX tumors and cultured in complete RPMI1640 medium plus 10 ng/ml EGF and 1% insulin-transferrin-selenium (ITS) as previously described [17]. All cells were cultured at 37 °C in a humidified incubator with 5% CO₂ and tested annually for mycoplasma contamination.

To establish THZ1-resistant cell line (MiaPaCa2-R), MiaPaCa-2 cells were exposed to a lower dose (10 nM) from the beginning. The concentration of THZ1 was increased until cells were able to proliferate normally in the presence of THZ1 of 100 nM.

Cell viability and colony formation assays

Cells were plated into 96-well plates in at least triplicate and then subjected to drug treatment as indicated for 72 h. Cell viability was then measured by using Celltiter Glo Assay (G7571, Promega). For colony formation assay, cells were plated into 6-well plate at indicated number. Cells were fixed with methanol and crystal violet staining was performed at the 7–10th day.

Cell cycle and apoptosis assays

Cell-cycle analysis was performed using the Cell Cycle staining kit (KGA511, KeyGEN Biotech). Cell apoptosis

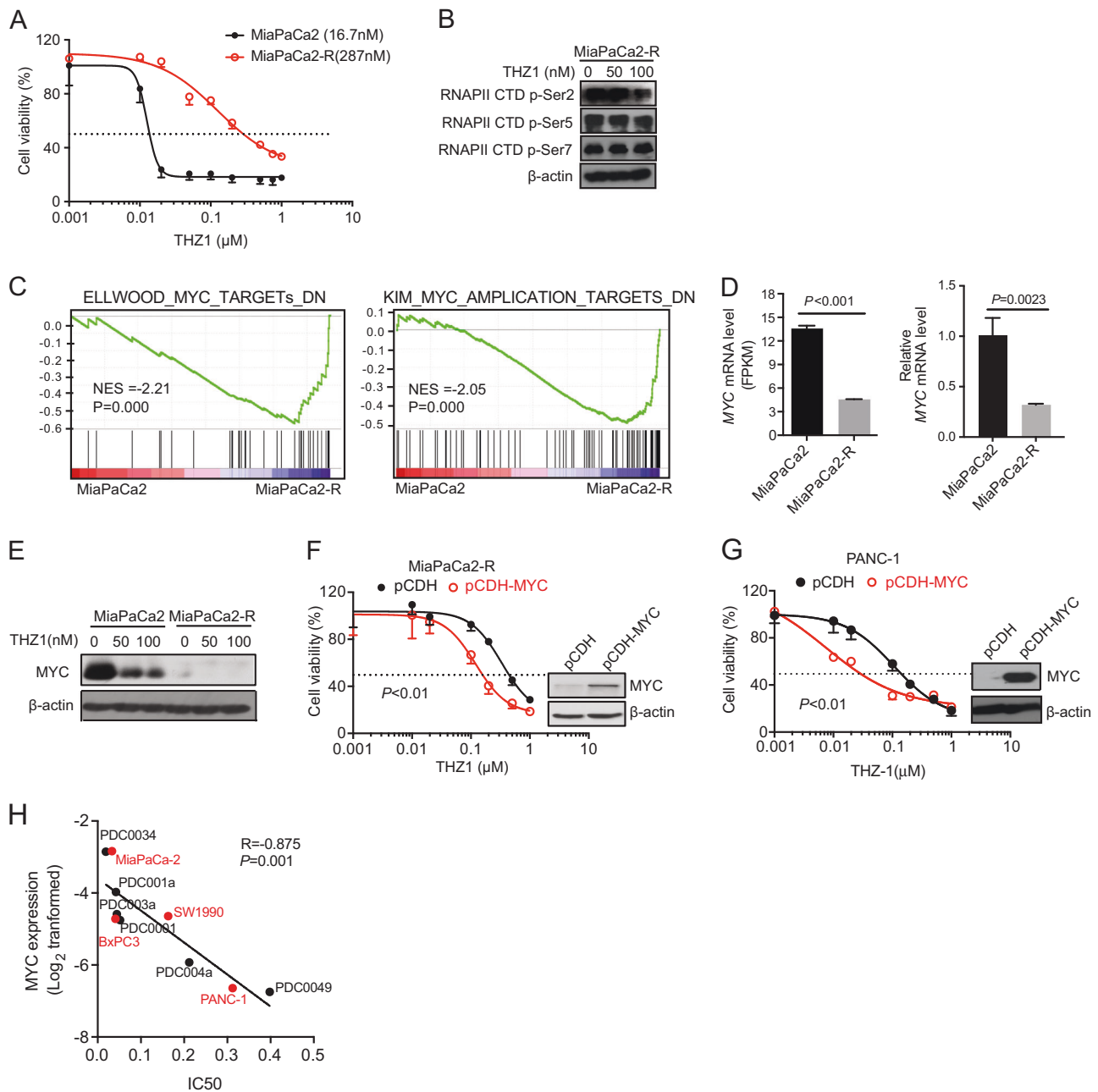


Fig. 6 MYC expression is associated with susceptibility of PDAC cells to THZ1. **a** Cell viability of MiaPaCa2 and MiaPaCa2-R after 72 h exposure to increasing dose of THZ1. Percentage of cell viability relative to that of DMSO-treated cells is shown. Data represent mean \pm SD of three replicates (two-way ANOVA). **b** Immunoblot analysis of the phosphorylation of RNAPII CTD, CDK7, and β -actin in MiaPaCa2 and MiaPaCa2-R cells treated with the indicated dose of THZ1 for 6 h. **c** Gene set enrichment analysis (GSEA) of MYC-downregulated gene sets were found to be enriched in MiaPaCa2-R

cells. **d** MYC mRNA expression from MiaPaCa2 and MiaPaCa2-R cells was shown as FPKM. **e** Immunoblot analysis of the MYC and β -actin in cells (MiaPaCa2 and MiaPaCa2-R) treated with the indicated dose of THZ1 for 6 h. **f, g** Cell viability comparison between MYC-expressing (pCDH-MYC) and control vector-expressing (pCDH) in MiaPaCa2-R or PANC-1, after 72 h treatment with increasing doses of THZ1. Results are means \pm SD of three replicates (Two-way ANOVA). **h** Relative mRNA level of MYC among PDC cells and PDAC cell lines were shown

was measured with Annexin V-FITC Apoptosis Detection Kit according to the manufacturer's protocol (KGA105, KeyGEN Biotech). The stained cells were acquired for analysis on LSRFortessa (BD), and data were analyzed with FlowJo software (Tree Star Inc.). For

caspase activity assay, cells were plated into 96-well plates in at least triplicates and then subjected to drug treatment as indicated. Cell caspase activity was then measured by using Caspase 3/7 glo assay (G8092, Promega).

Lentivirus preparation and infection

MYC or CDK7 sequence was cloned into pCDH vector carrying a puromycin resistance gene. As for CDK7 knockdown, sequence targeting CDK7 was cloned into Lenti-CRIPR-V2 vector. Sequences are listed as below: sgCDK7-1 For 5' -CACCGGAAGCTGGACTTCCTTGG GG-3', Rev 5'-AAACCCCAAGGAAGTCCAGCTTC C-3'; sgCDK7-2 For 5'-CACCGATCTCTGGCCTTGTAACGG-3', Rev 5'-AAACCCGTTTACAAGGCCAGAGATC-3'.

Lentiviruses were generated in HEK293T cells by transfecting cells using second-generation packaging vectors. Target cells were infected and selected using puromycin selection.

Immunoblot analysis

Cultured cells or tissues were extracted with RIPA buffer containing protease inhibitors and a phosphatase inhibitor cocktail (Roche). Protein concentration was determined by the BCA assay (Pierce). Proteins were resolved by SDS-PAGE, transferred to PVDF membrane (Millipore) and analyzed by immunoblot. Antibodies used were as follows: Phospho-RNAPII CTD(Ser2) (#13499), Phospho-RNAPII CTD(Ser5) (#13523), Phospho-RNAPII CTD(Ser7) (#13780), CDK7 (#2916), c-MYC (#605), Phospho-AKT (#4060), AKT (#2920), Phospho-p65 (#3033), p65(#8242), Phospho-STAT3 (#9134), STAT3 (#4904) were purchased from Cell Signaling Technology, β -actin (#A5316) from Sigma-Aldrich.

Quantitative RT-PCR

Total RNA was extracted by Trizol (Life Technologies) followed by cDNA synthesis with RevertAid First Strand cDNA Synthesis Kit (Thermo Scientific). Real-time qPCR was performed using SYBR Green qPCR Master Mix (Roche) in StepOnePlus System (ABI). Gapdh expression was used for normalization. The following primers were used: CDK7 For 5'-ATGGCTCTGGACGTGAAGTCT-3', Rev 5'-GCGACAATTTGGTTGGTGTTTC-3'; PLK1 For 5'-AAAGAGATCCCGGAGGTCCTA-3', Rev 5'-GGCTG CCGTGAATGGATATTTTC-3'; Cdc25c For 5'-TCTAC GGAACCTTCTCATCCAC-3', Rev 5'-TCCAGGAGCA GGTTTAACATTTT-3'; IKKKB For 5'-GGAAGTACC TGAACCAGTTTGAG-3', Rev 5'-GCAGGACGATGTT TTCTGGCT-3'; RelaA For 5'-ATGTGGAGATCAT TGAGCAGC-3', Rev 5'-CCTGGTCCTGTGTAGCCAT T-3'; Mcl1 For 5'-TGCTTCGGAAACTGGACATCA-3', Rev 5'-CCACAAAGGCACCAAAAAG-3'; BIRC3 For 5'-AAGCTACCTCTCAGCCTACTTT-3', Rev 5'-CCAC TGTTTTCTGTACCCGGA-3'; XIAP For 5'-GCTCC ACGAGTCCTACTGTG-3', Rev 5'-GTTCACTGCGACA

GACATCTC-3'; GAPDH For 5'-TGAAGTCAACAG CGACACCCA-3', Rev 5'-CACCCCTGTTGCTGTAGCCA AA-3'.

Histology and immunohistochemistry (IHC)

Tissue specimens were fixed in 10% buffered formalin and paraffin-embedded for histologic studies. Five micrometer of tissue sections were stained with hematoxylin and eosin (H&E), Ki67 (# ab16667, Abcam), cleaved Caspase 3 (#9661s, Cell Signaling Technology) and CK19 (#10712-1-AP, proteintech).

Patient-derived xenograft model and THZ1 treatment

Patient-derived xenografts from two patients (PDX0018 and PDX0088) were inoculated subcutaneously into 4-week-old female BALB/c (nu/nu) mice. Tumor volume was calculated using the formula: $V = 0.5 \times \text{length} \times \text{width} \times \text{width}$. When xenografts grow up to 100–150 mm³, mice were randomly divided into two groups, which were then treated with vehicle (DMSO in 5% dextrose), THZ1 (10 mg/kg in vehicle solutions) intraperitoneally twice daily. Tumor volume was measured every 2–3 days. Upon harvesting tumors, tumors were cut into half, with one-half fixed in formalin for histopathology analysis, and the other half fixed in RNALater for qRT-PCR analysis.

Pancreatic cancer mouse models and THZ1 treatment

Pancreatitis-induced tumorigenesis. Pancreatitis was induced at 6–8 weeks of age in male PDX^{cre} Kras^{+LSL-G12D} (KC) mice by administration of 6 hourly intraperitoneal (IP) injections of caerulein (50 μ g/kg, Sigma-Aldrich) over 1 week (three times per week). Mice were treated as indicated with THZ1 (10 mg/kg twice daily) or vehicle intraperitoneally. After 14 days, mice were killed and pancreata were collected for further studies.

Spontaneous model of pancreatic cancer. PDX^{cre} Kras^{+LSL-G12D} Trp53^{+LSL-R172H} (KPC) mice develop aggressive and quickly pancreatic cancer. Ten-weeks-old male KPC mice with fully developed PDAC were treated with Vehicle or THZ1 (10 mg/kg twice daily) intraperitoneally for 3 weeks. At the end of the experiment, pancreata were collected for further analysis.

All animals in the individual experiments were of the same age and sex. For each experiment, tumor-bearing mice were randomly assigned to the different treatment groups just prior to the start of treatment. In treatment studies where tumor growth was a critical outcome assessment of tumor size was performed blinded, by a second researcher.

Exclusion of data

Animals that never developed tumors due to take rate lower than 100% were excluded from the studies. All data from animals that died or had to be killed prior to the scheduled termination of the experiment was excluded.

RNA-Seq preparation and analysis

RNA sequencing service was supplied by SMARTQUERIER BIOTECH (Shanghai, China). Briefly, BxPC-3, Mia-PaCa-2, and PANC-1 treated with DMSO or THZ1 (100 nM) for 6 h were collected in biological triplicates. Total RNA was extracted and ERCC spike-in controls were added according to kit guidelines (Thermo 4456740). Libraries were constructed using TruSeq Stranded mRNA LTSample Prep Kit (Illumina) according to the manufacturer's instructions. Then these libraries were sequenced on the Illumina sequencing platform (HiSeq™ 2500 or Illumina HiSeq X Ten) and 125 bp/150 bp paired-end reads were generated. To adjust for global transcription shutdown by THZ1, the read count was normalized so that the ERCC spike-in read counts are the same in DMSO- and THZ1-treated sample [11]. The significantly differentially expressed genes (FDR \leq 0.05) were identified by ercc dashboard based on the normalized read count data per gene. For gene ontology analysis, the clusterProfiler was utilized to interrogate the molecular function ontology defined by the Gene Ontology Consortium. Sequencing and expression data have been deposited in the Gene Expression Omnibus under accession number GSE121273.

Study approval

Human pancreatic tissues from patients with pancreatic ductal adenocarcinoma were obtained from the Renji hospital with Local Ethics Committee approval and patient consents. All animal experiments were carried out following the guidelines of the Renji hospital institutional animal care and ethics committee.

Statistical analyses

Two-way ANOVA or one-way ANOVA together with Bonferroni's post hoc test was used for multiple groups analysis. Unpaired Student's *t*-test was used to determine statistical significance in the rest experiments, and *P*-value of less than 0.05 was considered significant. Values are expressed as mean \pm SEM or mean \pm SD (Prism 7; GraphPad Software). Unless indicated, results are from at least two- or three-independent experiments.

Author contributions J.X., P.L., and Y.T. designed experiment, interpreted data, and wrote the manuscript; P.L., J.G., and L.Z. performed most of the experiments; Y.W., N.N., and F.L. assisted in some experiments; Y.F., Y.-W.S., and Z.-G.Z. provided the key materials; J. X., Y.T. and L.-W.W. provided the overall guide.

Funding This work was supported by the Program for professor of Special Appointment (Eastern Scholar) at Shanghai Institutions of Higher Learning No.TP2015007 to J.X., TP2015017 to Y.T.), National Natural Science Foundation of China (81702938 and 81770628 to J.X.; 81572761 and 81772655 to Y.T.), Shanghai Municipal Education Commission-Gaofeng Clinical Medicine Grant Support No.20161312 (J.X.), The Recruitment Program of Global Experts of China (National 1000-Youth Talents Program to Y.T.), Shanghai Rising-Star Program (Y.T.).

Compliance with ethical standards

Conflict of interest The authors declare that they have no conflict of interest.

Publisher's note: Springer Nature remains neutral with regard to jurisdictional claims in published maps and institutional affiliations.

References

1. Yadav D, Lowenfels AB. The epidemiology of pancreatitis and pancreatic cancer. *Gastroenterology*. 2013;144:1252–61.
2. Edu CGAR. Integrated genomic characterization of pancreatic ductal adenocarcinoma. *Cancer Cell*. 2017;32:185.
3. Waddell N, Pajic M, Patch AM, Chang DK, Kassahn KS, Bailey P, et al. Whole genomes redefine the mutational landscape of pancreatic cancer. *Nature*. 2015;518:495–501.
4. Witkiewicz AK, Mcmillan EA, Balaji U, Baek G, Lin WC, Mansour J, et al. Whole-exome sequencing of pancreatic cancer defines genetic diversity and therapeutic targets. *Nat Commun*. 2015;6:6744.
5. Ryan DP, Hong TS, Bardeesy N. Pancreatic adenocarcinoma. *New Engl J Med*. 2014;371:1039.
6. Hidalgo M. Pancreatic cancer. *New Engl J Med*. 2010;362:1605–17.
7. Wang Y, Zhang T, Kwiatkowski N, Abraham BJ, Tong IL, Xie S, et al. CDK7-dependent transcriptional addiction in triple-negative breast. *Cancer Cell*. 2015;163:174.
8. Franco HL, Kraus WL. No driver behind the wheel? Targeting transcription in cancer. *Cell*. 2015;163:28–30.
9. Cao Kaixiang, Shilatifard Ali. Inhibit globally, act locally: CDK7 inhibitors in cancer therapy. *Cancer Cell*. 2014;26:158–59.
10. Kwiatkowski N, Zhang T, Rahl PB, Abraham BJ, Reddy J, Ficarro SB, et al. Targeting transcription regulation in cancer with a covalent CDK7 inhibitor. *Nature*. 2014;511:616–20.
11. Chipumuro E, Eugenio M, Camilla LC, Kwiatkowski N, Zhang T, Hatheway CM, et al. CDK7 inhibition suppresses super-enhancer-linked oncogenic transcription in MYCN-driven cancer. *Cell*. 2014;1126–39.
12. Christensen CL, Kwiatkowski N, Abraham BJ, Carretero J, Alshahrour F, Zhang T, et al. Targeting transcriptional addictions in small cell lung cancer with a covalent CDK7 inhibitor. *Cancer Cell*. 2014;26:909–22.
13. Jiang YY, Lin DC, Mayakonda A, Hazawa M, Ding LW, Chien WW, et al. Targeting super-enhancer-associated oncogenes in oesophageal squamous cell carcinoma. *Gut*. 2017;511:1358–68.

14. Yuan J, Jiang YY, Mayakonda A, Huang M, Ding LW, Lin H, et al. Super-enhancers promote transcriptional dysregulation in nasopharyngeal carcinoma. *Cancer Res.* 2017;77:6614–23.
15. Zhang Z, Peng H, Wang X, Yin X, Ma P, Jing Y, et al. Preclinical efficacy and molecular mechanism of targeting CDK7-dependent transcriptional addiction in ovarian cancer. *Mol Cancer Ther.* 2017;16:1739–50.
16. Wong R, Ngoc P, Leong WZ, Yam A, Zhang T, Asamitsu K, et al. Enhancer profiling identifies critical cancer genes and characterizes cell identity in adult T-cell leukemia. *Blood.* 2017;130:2326–38.
17. Wang X, Lu X, Zhang T, Wen C, Shi M, Tang X, et al. mir-329 restricts tumor growth by targeting grb2 in pancreatic cancer. *Oncotarget.* 2016;7:21441.
18. Hessmann E, Johnsen SA, Siveke JT, Ellenrieder V. Epigenetic treatment of pancreatic cancer: is there a therapeutic perspective on the horizon? *Gut.* 2017;66:168–79.
19. Mazur PK, Herner A, Mello SS, Wirth M, Hausmann S, Sánchez-Rivera FJ, et al. Combined inhibition of BET family proteins and histone deacetylases as a potential epigenetics-based therapy for pancreatic ductal adenocarcinoma. *Nat Med.* 2015;21:1163–71.
20. Garcia PL, Miller AL, Kreitzburg KM, Council LN, Gamblin TL, Christein JD, et al. The BET bromodomain inhibitor JQ1 suppresses growth of pancreatic ductal adenocarcinoma in patient-derived xenograft models. *Oncogene.* 2016;35:833–45.
21. Tang Z, Li C, Kang B, Gao G, Li C, Zhang Z. GEPIA: a web server for cancer and normal gene expression profiling and interactive analyses. *Nucleic Acids Res.* 2017;45:W98–W102.
22. Hidalgo M, Amant F, Biankin AV, Budinská E, Byrne AT, Caldas C, et al. Patient-derived xenograft models: an emerging platform for translational cancer research. *Cancer Discov.* 2014;4:998–1013.
23. Hingorani SR, Wang L, Multani AS, Combs C, Deramautd TB, Hruban RH, et al. Trp53R172H and KrasG12D cooperate to promote chromosomal instability and widely metastatic pancreatic ductal adenocarcinoma in mice. *Cancer Cell.* 2005;7:469–83.
24. Guerra C, Collado M, Navas C, Schuhmacher AJ, Hernández-Porrás I, Cañamero M, et al. Pancreatitis-induced inflammation contributes to pancreatic cancer by inhibiting oncogene-induced senescence. *Cancer Cell.* 2011;19:728–39.
25. Wong MH, Xue A, Julovi SM, Pavlakis N, Samra JS, Hugh TJ, et al. Cotargeting of epidermal growth factor receptor and PI3K overcomes PI3K-Akt oncogenic dependence in pancreatic ductal adenocarcinoma. *Clin Cancer Res.* 2014;20:4047–58.
26. Wu CY, Carpenter ES, Takeuchi KK, Halbrook CJ, Peverley LV, Bien H, et al. PI3K regulation of RAC1 is required for KRAS-induced pancreatic tumorigenesis in mice. *Gastroenterology.* 2014;147:1405–16.
27. Corcoran RB, Contino G, Deshpande V, Tzatsos A, Conrad C, Benes CH, et al. STAT3 plays a critical role in KRAS-induced pancreatic tumorigenesis. *Cancer Res.* 2015;71:5020–29.
28. Rachmilewitz M, Izak G, Hochman A, Aronovitch J, Grossowicz N. Critical role of NF- κ B in pancreatic cancer. *Oncotarget.* 2014;5:10969–75.
29. Lovén J, Orlando DA, Sigova AA, Lin CY, Rahl PB, Burge CB, et al. Revisiting global gene expression analysis. *Cell.* 2012;151:476–82.
30. Wang J, Hu K, Guo J, Cheng F, Jing L, Jiang W, et al. Suppression of KRas-mutant cancer through the combined inhibition of KRAS with PLK1 and ROCK. *Nat Commun.* 2016;7:11363.
31. Guo J, Kleeff J, Li J, Ding J, Hammer J, Zhao Y, et al. Expression and functional significance of CDC25B in human pancreatic ductal adenocarcinoma. *Oncogene.* 2004;23:71–81.
32. Ling J, Kang Y, Zhao R, Xia Q, Lee D, Chang Z, et al. Kras G12D -induced IKK2/ β /NF- κ B activation by IL-1 α and p62 feedforward loops is required for development of pancreatic ductal adenocarcinoma. *Cancer Cell.* 2012;21:105–20.
33. Ochiai T, Saito Y, Saitoh T, Dewan MZ, Shiyoa A, Kobayashi M, et al. Inhibition of IkappaB kinase beta restrains oncogenic proliferation of pancreatic cancer cells. *J Med Dent Sci.* 2008;55:49–59.
34. Gao Y, Zhang T, Terai H, Ficarro SB, Kwiatkowski N, Hao MF, et al. Overcoming resistance to the THZ series of covalent transcriptional CDK inhibitors. *Cell Chem Biol.* 2017;25:135–42.